Atmospheric
Chemistry
and Physics
Discussions

Open Access

Seasonal and interannual variations of HCN amounts in the upper troposphere and lower stratosphere observed by MIPAS

N. Glatthor[1], M. Höpfner[1], G. P. Stiller[1], T. von Clarmann[1], B. Funke[2], S. Lossow[1], E. Eckert[1], U. Grabowski[1], S. Kellmann[1], A. Linden[1], and A. Wiegele[1]

[1]Karlsruher Institut für Technologie, Institut für Meteorologie und Klimaforschung, Karlsruhe, Germany
[2]Instituto de Astrofísica de Andalucía (CSIC), Granada, Spain

ACPD

14, 8997–9040, 2014

Variations of MIPAS HCN amounts

N. Glatthor et al.

Title Page

Abstract	Introduction
Conclusions	References
Tables	Figures

|◄ ►|

◄ ►

Back Close

Full Screen / Esc

Printer-friendly Version

Interactive Discussion

Abstract

A global HCN dataset covering nearly the complete period June 2002 to April 2012 has been derived from FTIR limb emission spectra measured with the Michelson Interferometer for Passive Atmospheric Sounding (MIPAS) on the ENVISAT satellite. HCN is an almost unambiguous tracer of biomass burning with a tropospheric lifetime of 5–6 months and a stratospheric lifetime of about two years. We present a MIPAS HCN climatology with the main focus on biomass burning signatures in the upper troposphere and lower stratosphere. HCN observed by MIPAS in the southern tropical and subtropical upper troposphere has an annual cycle peaking in October–November during or shortly after the maximum of the southern hemispheric biomass burning season. Within 1–2 months after the burning season, a considerable portion of the enhanced HCN is transported southward to Antarctic latitudes. The fundamental period in the northern upper troposphere is also an annual cycle, which in the tropics peaks in May after the biomass burning seasons in northern tropical Africa and South Asia, and in the subtropics in July due to trapping of pollutants in the Asian monsoon anticyclone. However, caused by extensive biomass burning in Indonesia and Northern Africa together with northward transport of parts of the southern hemispheric plume, in several years HCN maxima are also found around October/November, which leads to semi-annual cycles in the northern tropics and subtropics. Because of overlap of interannually varying burning activities in different source regions, both southern and northern low-latitude maxima have considerable interannual variations. There is also a temporal shift between enhanced HCN in northern low and mid-to-high latitudes, indicating northward transport of pollutants. Due to additional biomass burning at mid and high latitudes this meridional transport pattern is not as clear as in the Southern Hemisphere. Presumably caused by ocean uptake, upper tropospheric HCN above the tropical oceans decreases to below 200 pptv especially during boreal winter and spring. HCN time series at 10 km altitude indicate a negative trend, which is more distinct in the northern (-1.3 to $-2.1\%\,yr^{-1}$) than in the Southern Hemisphere (-0.1 to $-0.7\%\,yr^{-1}$). The trop-

Variations of MIPAS HCN amounts

N. Glatthor et al.

ical stratospheric tape recorder signal with an apparently biennial period, which has been detected in MLS and ACE-FTS data from mid-2004 to mid-2007, is corroborated by MIPAS HCN data. The tape recorder signal in the whole MIPAS dataset exhibits periodicities of 2 and 4 yr, generated by interannual variations in biomass burning. The strongest positive anomaly in the year 2007 is caused by superposition of enhanced HCN from southern hemispheric and Indonesian biomass burning at the end of the year 2006 and from African sources in spring and the Asian monsoon during summer. The vertical transport time of the anomalies is 1 month or less between 14 and 17 km in the upper troposphere and about 9 months between 17 and 25 km in the lower stratosphere.

1 Introduction

Hydrogen cyanide (HCN) is one of the most abundant atmospheric cyanides (Singh et al., 2003). The first spectroscopic detection of stratospheric HCN was reported by Coffey et al. (1981), and the first discovery of tropospheric HCN by Rinsland et al. (1982). Model calculations by Cicerone and Zellner (1983) resulted in rather uniform tropospheric HCN concentrations, which slowly decreased with altitude in the stratosphere. They identified oxidation with OH as main tropospheric sink and reaction with $O^1(D)$ and photodissociation as major stratospheric sinks, resulting in an atmospheric residence time of about 2.5 yr. However, various measurements performed in the 1990s (Mahieu et al., 1995, 1997; Rinsland et al., 1998, 1999, 2000, 2001a, b, 2002) showed that tropospheric HCN exhibits strong seasonal and spatial variations, which is inconsistent with a tropospheric lifetime of several years. These observations led to the conclusion that biomass burning is a major source of atmospheric HCN and that there must be an additional sink of tropospheric HCN. Today, HCN is considered as an almost unique tracer of biomass burning (Li et al., 2003; Singh et al., 2003; Yokelson et al., 2007; Lupu et al., 2009) and ocean uptake is assumed to be the major sink,

leading to a tropospheric lifetime of 5–6 months (Li et al., 2000, 2003; Singh et al., 2003).

HCN released by extensive biomass burning can form persistent upper tropospheric plumes, e.g. the southern hemispheric biomass burning plume caused by continuous combustion throughout the dry season in South America, central and southern Africa and Australia, which regularly peaks between September and November. The spatial extension and composition of this plume has been investigated using various ground based, airborne and spaceborne observations (Singh et al., 1996, 2000; Rinsland et al., 2001, 2005; von Clarmann et al., 2007; Glatthor et al., 2009). Another region of enhanced upper tropospheric HCN is the Asian monsoon anticyclone, which is centered above southern Asia in June, July and August (Park et al., 2008). Spaceborne observations of global HCN have been performed by the Fourier Transform Spectrometer of the Atmospheric Chemistry Experiment (ACE-FTS) (Rinsland et al., 2005) and, generally restricted to the middle atmosphere, by the Microwave Limb Sounder (MLS) on the Aura satellite (Pumphrey et al., 2006). Climatologies of the HCN distribution obtained by ACE-FTS have been presented by Lupu et al. (2009) and Randel et al. (2010).

Transport of tropospheric trace gases into the stratosphere mainly occurs at the tropical tropopause (Holton et al., 1995). If a tropospheric source gas exhibits a temporal variation, this feature will propagate into the stratosphere and be transported upward by the Brewer–Dobson circulation with a temporal lag, which increases with altitude. This phase shift is called tropical tape recorder and has been observed in water vapour, CO_2 and CO (Mote et al., 1996; Andrews et al., 1999; Schoeberl et al., 2006). First observations of a HCN tape recorder signal in data of the Microwave Limb Sounder (MLS) on the Aura satellite and of the Atmospheric Chemistry Instrument (ACE-FTS) on SCISAT-1 were published by Pumphrey et al. (2008). These authors analysed the period July 2004 to June 2007 and found a period of 2 yr, which is in contrast to the annual cycle of the tape recorder signals of water vapour, CO_2 and CO. They state that the reason for the 2 year cycle is not fully understood and suggest that it might be due to interannual variations in biomass burning in Indonesia. In subsequent pub-

Title Page

Abstract | Introduction

Conclusions | References

Tables | Figures

◄ | ►

◄ | ►

Back | Close

Full Screen / Esc

Printer-friendly Version

Interactive Discussion

lications these observations were compared with model runs. Li et al. (2009) used ground based column measurements as well as MLS and ACE-FTS data to constrain the GEOS-Chem model and found consecutive 2 year cycles of the HCN anomaly in the lower stratosphere. They argued that the 2 year tape recorder cycle is caused by the extent of temporal overlap of biomass burning in Africa and other regions. Pommrich et al. (2010) were able to reproduce the observed 2 year tape recorder signal with the Chemical Lagrangian Model of the Stratosphere (CLaMS) by use of temporally resolved biomass burning emissions from Indonesia, but they expected an irregular cycle for a longer time series. Thus the question whether there is a periodicity in the HCN tape recorder signal is still open, and the long time series of MIPAS data is well suited to bring more insight into this problem.

In the following we will shortly describe the MIPAS instrument and the HCN retrieval setup. In the discussion we will at first show a seasonal climatology of the HCN distribution of the whole measurement period of MIPAS and compare the MIPAS results with a HCN climatology established from ACE-FTS v2.2 data. Then, by presenting time series of zonal averages of MIPAS HCN data of the upper troposphere we will show, that there are considerable interannual differences between the seasonal patterns. By presentation of monthly global distributions we will illustrate the reasons for interannual differences. Finally, we will present the HCN tape recorder signal obtained from the whole MIPAS dataset.

2 MIPAS measurements

2.1 Instrument description

The Michelson Interferometer for Passive Atmospheric Sounding (MIPAS) has been operated onboard the European ENVIronmental SATellite (ENVISAT), which was launched into a Sun-synchronous polar orbit at about 800 km altitude on 1 March 2002. The satellite's equator crossing times are ~ 10:00 LT and ~ 22:00 LT. MIPAS is a limb-

viewing Fourier transform infrared (FTIR) emission spectrometer covering the mid-infrared spectral region between 685 and 2410 cm^{-1} (4.1–14.6 μm), which enables simultaneous observation of numerous trace gases (European Space Agency (ESA), 2000, Fischer et al., 2008). MIPAS data have been transmitted from June 2002 until April 2012, when the communication to ENVISAT was lost.

From June 2002 to April 2004 MIPAS has been operated in its original high resolution (HR) mode with a spectral resolution of 0.025 cm^{-1} and a latitudinal sampling distance of ∼ 4.8° (530 km). After a data gap due to technical problems, MIPAS was run in the so-called reduced resolution (RR) measurement mode with a spectral resolution of 0.0625 cm^{-1} and a latitudinal sampling distance of ∼ 3.6° (400 km) since January 2005. We present data of the HR and of the RR "nominal" measurement modes, consisting of rearward limb-scans covering the altitude region between 7 and 72 km within 17 and 27 altitude steps, respectively. The step-width of the HR mode was 3 km up to 42 km and 5 to 8 km at higher altitudes. The step-width of the RR "nominal" mode was 1.5 km up to 22 km, 2 km up to 32 km, 3 km up to 44 km and 4–4.5 km for the upper part of the scan. MIPAS was able to measure during day and night, and produced up to 1000 scans per day in original mode and up to 1400 scans per day in RR nominal mode. The level-1B radiance spectra used for retrieval are data version 5.02/5.06 (reprocessed data) provided by the European Space Agency (ESA) (Nett et al., 2002).

2.2 Retrieval method and error estimation

We present HCN distributions measured by MIPAS-ENVISAT. The respective data versions are V5H_HCN_20 of the MIPAS HR mode and V5R_HCN_220 of the MIPAS RR mode. Processing of MIPAS data at IMK has been described in various papers (von Clarmann et al., 2003; Höpfner et al., 2004). Retrieval of HCN from MIPAS RR-spectra has been described by Wiegele et al. (2012). For reasons of consistency the retrieval setup of the MIPAS HR dataset presented here has been adjusted to the MIPAS RR retrieval setup, and is different from the setup discussed in Glatthor et al. (2009).

Retrievals were performed with the processor of the Institut für Meteorologie und Klimaforschung and the Instituto de Astrofísica de Andalucía (IMK/IAA), using the Karlsruhe Optimized and Precise Radiative Algorithm (KOPRA) (Stiller, 2000) for radiative transfer calculations and the Retrieval Control Program (RCP) of IMK/IAA for inverse modelling. The HCN datasets V3O_HCN_2 derived from MIPAS HR spectra presented in Glatthor et al. (2009) had been retrieved in 10 microwindows covering the spectral range 715.5–782.75 cm^{-1}. For analysis of the reduced resolution data, these microwindows were slightly extended to match the wider wavenumber grid and some of them were not applied in the stratosphere. The inversion consists of derivation of vertical profiles of atmospheric state parameters from MIPAS level-1B spectra by constrained non-linear least squares fitting in a global-fit approach (von Clarmann et al., 2003). Since the retrieval grid chosen has a finer altitude spacing than the height distance between the tangent altitudes, a constraint is necessary to attenuate instabilities. For this purpose, Tikhonov's first derivative operator was applied (Steck, 2002, and references therein). Instead of climatological HCN a-priori profiles, height-constant profiles were chosen to avoid any influence of the a-priori information on the shape of the retrieved profiles. HCN retrieval from HR spectra was performed without joint-fitting of interfering gases. The radiative contribution of these gases was modelled by using their profiles as retrieved earlier in the processing sequence. For retrieval of HCN from spectra of the RR-period the constraint was weakened by a factor of two, and ozone was joint-fitted to further improve the fit, but all other interfering gases were also modelled using their prefitted profiles. These changes as well as the modified microwindow setup were also applied for creation of the updated HCN dataset V5H_HCN_20 of the MIPAS HR period. For both measurement periods additional retrieval parameters were microwindow-dependent continuum radiation profiles and microwindow-dependent, but height-independent zero-level calibration corrections. When no prefitted profiles were available, we used the data of the MIPAS climatology (Remedios et al., 2007). MIPAS single scan measurements provide information on atmospheric HCN from the lower end of the profiles in the free troposphere up to about 45 km altitude. The total HCN

retrieval error for a single MIPAS scan observing a tropospheric biomass plume burning plume is 12–15 % in the upper troposphere and 18–22 % in the lower and middle stratosphere. The vertical resolution is 4–5 km in the troposphere and 6–8 km in the stratosphere.

3 Discussion of the HCN dataset

3.1 Seasonal climatology

Figure 1 shows latitude-height cross sections of MIPAS HCN volume mixing ratios (VMRs) measured in spring, summer, fall and winter, averaged over the whole measurement period 2002–2012. Averaging was performed for $7.5° \times 1$ km latitude–altitude bins at the poles and $5° \times 1$ km latitude–altitude bins elsewhere. Above 10 km altitude the averages are generally based on 10 000–15 000 values. Due to cloud-contamination and to the upward-shift of the MIPAS RR mode scans towards low latitudes, increasingly less data points could be binned at 10 km and below, e.g., only some dozens or even less than 10 values at 7 km altitude in the tropics. For this reason and to avoid predominance of MIPAS HR data (latitude independent scans starting at 6 km), these regions are masked as white areas in the climatology. The standard deviation of the mean values is less than 1 pptv in the stratosphere, less than 2 pptv in the upper troposphere and increases up to about 8 pptv at 10 km altitude in the tropics. During all seasons the background HCN amounts in the undisturbed upper troposphere and lower stratosphere (UTLS) are between 200 and 280 pptv (green areas).

From March to May (top left) there are enhanced tropospheric values of more than 350 pptv at northern subtropical to polar latitudes, caused by biomass burning in northern tropics to mid-latitudes. Near $20°$ N the HCN plume extends up to 15 km altitude. The enhanced values above the Antarctic are pollutants released by southern hemispheric biomass burning during previous autumn, which have subsequently been transported southward (cf. Sect. 3.3). The lowest tropospheric values of below 200 pptv ap-

pear at southern tropical and subtropical latitudes. This minimum is probably caused by ocean uptake (cf. Li et al., 2000, 2003) during a long period without southern hemispheric biomass burning. Because of its long middle-atmospheric lifetime of 2.5 yr (Cicerone and Zellner, 1983), stratospheric HCN acts as dynamic tracer like CH_4, N_2O or various CFCs and is able to map seasonal cycles. There is a general decrease of HCN with altitude and towards high latitudes. The lowest stratospheric HCN amounts of less than 100 pptv occur at high latitudes, reflecting subsidence from higher altitudes in the early Antarctic and late northern vortex.

The latitude-height cross section of the summer period (top right) exhibits more enhanced HCN amounts below 10 km in northern mid- to polar latitudes than in spring, showing intensified biomass burning. Due to trapping of pollutants in the Asian monsoon anticyclone (AMA) (cf. Fig. 2), the size and strength of the HCN plume in the northern subtropics has considerably increased, extending from 20° N to 50° N and up to 17 km altitude. At 15 km it reaches southward as far as 10° N. Compared to the previous season the tropospheric minimum at low latitudes is somewhat attenuated and now covers the northern and southern tropics, while the HCN amounts at Antarctic latitudes have decreased to background values. Stratospheric HCN reflects the fully developed Antarctic vortex.

While during spring and summer enhanced tropospheric HCN has mainly been observed in the Northern Hemisphere, the autumn cross section (bottom left) exhibits a large area of enhanced HCN amounts of up to more than 400 pptv covering the southern tropics and mid-latitudes. This strong signature is caused by intensive southern hemispheric biomass burning. The plume extends up to 17 km altitude in the subtropics and up to 8 km at high southern latitudes. At 13–16 km altitude it stretchs northward across the Equator, where it is captured by the northern subtropical jet and further distributed up to 20° N (cf. Fig. 2). The low-latitude tropospheric HCN minimum is now shifted towards the northern tropics and subtropics, but less pronounced than in the previous seasons.

Title Page

Abstract | Introduction

Conclusions | References

Tables | Figures

|◄ | ►|

◄ | ►

Back | Close

Full Screen / Esc

Printer-friendly Version

Interactive Discussion

The winter cross section (bottom right) contains least enhanced HCN in the northern troposphere, reflecting interruption of biomass burning, and a re-strengthened minimum at tropical latitudes. The enhanced HCN amounts observed at mid to high southern latitudes are remnants of the southern hemispheric biomass burning plume of the preceding fire-season, which have been transported southward. Transport of pollutants towards high southern latitudes is supported by ground-based FTIR observations (Zeng et al., 2012). Due to subsidence in the Arctic vortex, stratospheric HCN is lowest at high northern latitudes.

To give an overview of the horizontal distribution of climatological HCN with the focus on the tropical and subtropical upper troposphere, Fig. 2 shows the seasonal variation at 14 km altitude. Boreal spring (top left) is characterised by biomass burning in western and northern tropical Africa, forming a plume, which covers the whole tropical Africa and parts of the surrounding oceans. The northern part of this African plume is transported over South Asia as far as to the eastern Pacific by the northern subtropical jet. This feature becomes even more obvious in a climatology restricted to the month of May, where enhanced amounts of HCN prevail in the whole northern subtropics (cf. Fig. 7). The HCN amounts observed above the southern tropical Pacific and the southern Atlantic are very low, which as mentioned above indicates ocean uptake. The main feature during boreal summer (top right) is considerably enhanced HCN in the whole AMA region. Due to initiated biomass burning, the HCN amounts above the tropical oceans have somewhat increased. The most extensive biomass burning plume is observed in the southern tropics and subtropics during September to November (bottom left), extending from South America over southern Africa to Australia and, driven by the southern subtropical jet, further around the globe above the southern tropical Pacific. A smaller part of the polluted air masses is obviously transported northeastward from Africa over South Asia to the northern Pacific. There is only a weak feature of biomass burning in Indonesia and tropical Australia in this climatology, which is due to the sporadic occurrence of this process. Because of strong biomass burning the size of the minimum above the tropical oceans is smallest in this season. During boreal winter

the southern hemispheric plume still covers nearly the same area as in the preceding season, but is considerably diluted. Strongly enhanced HCN amounts are restricted to the area above the southern tropical and subtropical Atlantic as well as southern and northeastern Africa. A certain part of the plume has spread into southern mid-latitudes.

Plume expansion to high southern latitudes can not be seen at this altitude, which is stratospheric over the Antarctic.

In Fig. 3 we present a monthly climatology of HCN observed by MIPAS at 10, 14, 18 and 22 km altitude in six different latitude bands. Generally, the altitude of 10 km is tropospheric at low to mid-latitudes, but in the tropopause region at high latitudes. The altitude of 14 km is tropospheric in the tropics and subtropics but stratospheric at mid and high latitudes, whereas the altitudes of 18 and 22 km are stratospheric at all latitudes. The midlatitude and tropical HCN amounts at 22 km altitude are between 200 and 220 pptv and exhibit nearly no annual variation. Due to subsidence in the polar vortices the respective curves from high latitudes show seasonal variations, with minimum values as low as 140 pptv in the Antarctic vortex. The HCN amounts at 18 km are 40–60 pptv higher than at 22 km and vary in a similar manner. The curves at 10 and 14 km altitude reflect the seasonality of global biomass burning. The summer maxima at 10 km at northern mid- and high latitudes are caused by boreal biomass burning and partly by northward transport of pollutants released at lower latitudes. In the northern tropics and subtropics there is a maximum of 340 pptv at 10 km in May and a somewhat weaker maximum at 14 km in June, caused by springtime biomass burning and by trapping of pollutants in the uppermost troposphere in the Asian monsoon anticyclone. The lowest HCN amounts of less than 250 pptv of this latitude band were observed in February. The strongest signatures of biomass burning and largest seasonal amplitudes occur at southern low and mid-latitudes. The maximum values at 10 km are 420 pptv in the latitude band 0–30° S during October and 380 pptv in the latitude band 30–60° S during November, followed by a considerable decrease in December. At 14 km, the southern tropical and subtropical maximum is slightly weaker and shifted towards November, while the southern midlatitude maximum is considerably reduced

Title Page

Abstract | Introduction

Conclusions | References

Tables | Figures

◀ | ▶|

◀ | ▶

Back | Close

Full Screen / Esc

Printer-friendly Version

Interactive Discussion

and further delayed until December. At this altitude overlap with stratospheric contributions gains influence. Minimum HCN values measured in these latitude bands at 10 km altitude were 200 pptv in April and 230 pptv in May, respectively. Due to poleward transport of polluted southern hemispheric air masses there is an increase of Antarctic HCN at 10 km of up to 340 pptv during November to January, which subsequently decreases to 250 pptv in May.

3.2 Comparison to ACE-FTS

A qualitative comparison of MIPAS HCN data can be performed with the HCN climatologies derived from measurements of the Fourier Transform Spectrometer of the Atmospheric Chemistry Experiment (ACE-FTS) on SCISAT (Lupu et al., 2009; Randel et al., 2010). Generally, the ACE-FTS distribution exhibits a similar latitudinal and seasonal variation as measured by MIPAS. During boreal spring ACE-FTS also observed a plume in the northern tropics and subtropics and moderately enhanced HCN amounts at northern mid-latitudes. Boreal summer is characterised by the plume inside the Asian monsoon anticyclone and intensified biomass burning at northern mid- to high latitudes. The highest seasonal tropospheric HCN amounts were also measured between September and November in a large area at southern hemispheric low- to mid-latitudes (Randel et al., 2010, Figs. S1 and S2). Further, ACE-FTS also measured very low HCN amounts over the tropical and subtropical oceans, especially during boreal winter, spring and summer and a poleward transport of enhanced HCN during or after the southern hemispheric biomass burning season (Lupu et al., 2009, Fig. 4; Randel et al., 2010, Figs. 1, S1 and S2).

However, there are also differences: the HCN background values measured by MIPAS at 13–14 km are between 250 and 300 pptv, while those of ACE-FTS measured at 13.5 km obviously range between 200 and 250 pptv only (Lupu et al., 2009, Fig. 5; Randel et al., 2010, Fig. S2). The HCN minimum observed by ACE-FTS over the tropical Pacific (Randel et al., 2010, Figs. 1 and S1) is lower than the minimum derived from MIPAS data. Further, different to MIPAS observations, the climatological AMA plume

Title Page

Abstract | Introduction

Conclusions | References

Tables | Figures

◀ | ▶

◀ | ▶

Back | Close

Full Screen / Esc

Printer-friendly Version

Interactive Discussion

extends considerably higher into the lower stratosphere than the southern hemispheric plume (Randel et al., 2010, Figs. 2 and S2).

To a certain extent, deviations between the MIPAS and ACE-FTS HCN climatologies can arise from different underlying time periods and from the lower spatio-temporal coverage of the ACE-FTS data as compared to the MIPAS distributions. Another possible reason for deviations is the use of different spectral bands for retrieval. The spectral regions used for ACE-FTS HCN retrievals are 1395–1460 and 3260–3355 cm^{-1} (Lupu et al., 2009), while for MIPAS HCN retrievals microwindows between 715 and 783 cm^{-1} are used.

A systematic bias between HCN VMRs of MIPAS and ACE-FTS can hence not be excluded. Associated uncertainties, however, have only little implications for the following discussion, focusing on seasonal and interannual variations.

3.3 Time series

To illustrate interannual variations, Fig. 4 shows time series of monthly zonal averages of HCN at 10, 14, 18 and 22 km altitude covering the operational period of MIPAS from June 2002 to April 2012. These altitudes have been chosen to cover the tropical and subtropical upper troposphere and lowermost stratosphere. Averaging was performed for 7.5°-latitude bins at the poles and 5°-latitude bins elsewhere, which generally resulted in adding up of several hundred to more than thousand values at the altitude of 10 km and above. Only at high latitudes and low altitudes less values were binned during winter and spring, e.g. 10–15 values at 10 km. As already shown in Fig. 1, the most significant signatures of biomass burning are visible in the southern hemispheric tropical and subtropical upper troposphere (top row). In this region the HCN distribution exhibits a clear annual cycle with maxima in October–November during or shortly after the peak of southern hemispheric biomass burning and minima during boreal spring. The magnitude of the maxima at 10 and 14 km varies considerably between 300 and more than 500 pptv. Especially strong southern hemispheric biomass burning plumes were observed at the end of the years 2002 and 2006 and particularly weak plumes in

Title Page

Abstract | Introduction

Conclusions | References

Tables | Figures

|◄ | ►|

◄ | ►

Back | Close

Full Screen / Esc

Printer-friendly Version

Interactive Discussion

the years 2003 and 2008. The time series at 10 km shows the transport of enhanced HCN to high southern latitudes within ~ 2 months after the peaks of the biomass burning seasons. Additional sources of HCN at southern mid- to high latitudes leading to an apparent meridional transport pattern only can be excluded. Poleward transport of considerable amounts of southern hemispheric biomass burning products is confirmed by time series of ground-based FTIR measurements of CO, HCN and C_2H_6 above Lauder (New Zealand) and Arrival Heights (Antarctica) presented by Zeng et al. (2012), which regularly peak at the end or some weeks after the southern hemispheric biomass burning season.

Significant signatures of biomass burning are also visible in the northern tropical and subtropical troposphere. The underlying period in this region is also an annual cycle with maxima around May in the tropics and around July in the subtropics, i.e. during the biomass burning seasons in South Asia and northern Africa and the peak of the Asian monsoon period, respectively. However, especially at 14 km, there are additional peaks at the end of the years 2002, 2006, 2010 and 2011 caused by strong biomass burning in Indonesia, northern tropical Africa and by northward effusion from the southern hemispheric plume (cf. Sect. 3.1), leading to semi-annual cycles during these periods. These peaks are closely connected across the equator with the southern hemispheric maxima. The reason for enhanced burning during the years 2002 and 2006 is a strong positive phase of the so-called El Niño-Southern Oscillation (ENSO) (http://jisao.washington.edu/datasets/globalsstenso/), characterised by drought periods in Indonesia. These features will be investigated in more detail in Sect. 3.4. Enhanced HCN is obviously also transported to higher northern latitudes, but the transport pattern is not as clear as in the Southern Hemisphere due to additional biomass burning at northern mid-latitudes during summer.

At the altitude of 18 km the tropical and subtropical annual and semi-annual cycles are considerably reduced (bottom left). The distribution at this altitude gives information about transport of enhanced HCN into the stratosphere. The time from end of 2006 until end of 2007 was the most effective period, characterised by upward transport of

Title Page

Abstract | Introduction

Conclusions | References

Tables | Figures

|◄ | ►|

◄ | ►

Back | Close

Full Screen / Esc

Printer-friendly Version

Interactive Discussion

enhanced HCN in the southern hemispheric and Indonesian biomass burning plumes at the end of 2006, above Africa in spring 2007 and in the strongly polluted AMA during summer 2007 (cf. Sect. 3.4). The combination of the same three sources is most likely responsible for the features of enhanced HCN observed from end of 2002 until end of 2003 and from end of 2010 until end of 2011. During the years 2008–2010 lower amounts of HCN were observed in the tropical and subtropical lowermost stratosphere. The interannual variation of the HCN release into the stratosphere becomes even more evident at 22 km altitude (bottom right), where the tropical HCN distribution exhibits maxima from beginning of 2003 to 2004, from mid-2005 to mid-2006, from early 2007 to fall 2008 and from 2011 to 2012. In general, entry of enhanced HCN into the lower stratosphere seems to be somewhat more effective in the northern than in the Southern Hemisphere, but the dominance of the Asian Monsoon is not as distinct as shown by Randel et al. (2010, Fig. 3).

For better quantification of meridional transport times, Fig. 5 shows monthly zonal averages of HCN VMRs at 10 km altitude for the latitude bands 0–30°, 30–60° and 60–90°, both for the Northern and Southern Hemisphere. In the Southern Hemisphere (right) there is a rather clear transport pattern. Meridional transport times can be estimated from the shifts between the HCN maxima at southern (sub)tropical and polar latitudes. The shifts vary between 0 months in the year 2008 and 2–3 months in the years 2002 and 2006, with an average value of ∼ 1.6 months (cf. Table 1). For comparison, the transport time for CO columns measured in New Zealand and in the Antarctic derived by Morgenstern et al. (2012) from correlation analysis is 15–40 days. A likely reason for the scatter of the estimated HCN transport times is the interannual latitudinal variation of the focal point of biomass burning. In 2002 and 2006 a considerable portion of biomass burning occurred in the inner tropics leading to longer poleward transport times, whereas in 2008 the HCN maximum at 10 km altitude was located further south in the subtropics and there was nearly no contribution from the tropics. As evident from Fig. 4, estimation of poleward transport times is more difficult in the Northern Hemisphere due to additional biomass burning at mid-latitudes and semi-annual variations

(Fig. 5, left). The only period with a transport pattern similar to the Southern Hemisphere is the year 2003, for which a time shift of 3 months between the tropical and polar HCN maximum can be derived. All other years are obviously disturbed by the two additional effects just mentioned.

The dotted lines in Fig. 5 show the results of a linear regression analysis of the temporal evolution of the HCN amounts in the different latitude bands. To avoid distortion by transition from MIPAS high to reduced resolution measurement mode, the analysis was performed for the latter measurement mode covering the period January 2005 to April 2012 only. The northern hemispheric trends are between -1.3 and $-2.1\,\%\,\mathrm{yr}^{-1}$, while the southern hemispheric trends are considerably weaker, namely between -0.1 and $-0.7\,\%\,\mathrm{yr}^{-1}$. A negative trend of about $-1\,\%\,\mathrm{yr}^{-1}$ for the period 2000–2012 has also been found by Worden et al. (2013) for tropospheric northern hemispheric CO, which is another, although not unique, tracer of biomass burning. Zeng et al. (2012) report on negative trends of $(-0.93 \pm 0.47)\,\%\,\mathrm{yr}^{-1}$ and $(-1.41 \pm 0.71)\,\%\,\mathrm{yr}^{-1}$ in HCN columns measured between 1998 and 2009 in the Southern Hemisphere above Lauder and Arrival Heights. Future analysis will address the significance of MIPAS HCN trends in more detail.

3.4 Reasons for interannual variations

3.4.1 The southern hemispheric biomass burning plume

To investigate the reasons for interannual variations of the strength of the southern hemispheric maxima (Figs. 4 and 5) in more detail, we compare global monthly HCN distributions of October and November at 14 km altitude of four different years (Fig. 6). Averaging was performed for $7.5° \times 15°$ latitude–longitude bins at the poles and $5° \times 15°$ latitude–longitude bins elsewhere.

The upper row shows the development of the extensive plume of the year 2002. In October, the focal points of biomass burning were above northern Australia and Indonesia, leading to averages of up to 700 pptv in this region, and above the southern

tropical Atlantic. Enhanced HCN amounts already covered the whole southern subtropical latitude band. In November intensified biomass burning obviously occurred in South America, southern and central Africa, which caused another strong plume extending from South America over southern Africa towards Australia. In both months, a certain part of the pollutants was transported above the northern tropical Indian Ocean towards South Asia. Thus, the contiguous area of enhanced HCN extending from the southern subtropics over the equator into the northern subtropics in the time series in Fig. 4, obviously was caused by sources in South America, southern Africa and additionally strong biomass burning in Indonesia and Eastern Africa. The above-average strength of the southern hemispheric plume of the year 2002 is confirmed by a time series of HCN emissions of the Global Fire Emissions Database-v2 (GFEDv2, van der Werf et al., 2006), which exhibits high biomass burning emissions in Indonesia and Australia in fall 2002 (Li et al., 2009, Fig. 8). Further, model calculations of Zeng et al. (2012) using emissions of the GFEDv3 database (van der Werf et al., 2010) to simulate the HCN release show an above-average biomass burning effect on HCN above Lauder (New Zealand) for 2002.

In 2003 MIPAS observed the weakest plume of its measurement period (second row). HCN amounts of 350 pptv and above covered the southern tropical and subtropical Atlantic, southern Africa and parts of the Indian Ocean only. In this year no biomass burning signatures from Indonesia and Australia were detected. Instead, the HCN amounts observed above Indonesia and the tropical Pacific decreased to 200 pptv or below, which probably reflected ocean uptake as proposed by Li et al. (2000, 2003). Further, there was also less burning activity in South America and southern Africa leading to maximum monthly means of 400–450 pptv only. The weak plume of 2003 is consistent with low GFEDv2 biomass burning emissions (Li et al., 2009, Fig. 8) and model calculations presented in Zeng et al. (2012), which for this year show an average biomass burning signature at Lauder only.

Another very strong southern hemispheric HCN plume was detected in the year 2006 (third row). This observation is confirmed by model calculations of tropospheric HCN

Full Screen / Esc

Printer-friendly Version

Interactive Discussion

columns above Lauder by Zeng et al. (2012), in which the biomass burning signature of the year 2006 turned out to be the strongest of the period 2002–2009. In October the plume was most distinct above the Indian Ocean, caused by strong biomass burning in Indonesia. This feature is in good agreement with the CO distribution obtained during the same month by the Microwave Limb Sounder (MLS) on the Aura satellite at the 147 hPa level (∼ 14 km) (Liu et al., 2013, Fig. 8b). In November there was an even more distinct maximum above and around Indonesia, extending considerably into the Northern Hemisphere, and another "hot spot" above Eastern Africa. Further, there were strongly enhanced HCN amounts in the whole subtropical latitude band. Again, the huge maximum above Indonesia is consistent with GFEDv2 emissions presented by Li et al. (2009) and GEOS-Chem model calculations for CO using GFED v2 and v3 emissions (Liu et al., 2013). Like in 2002, overlap of emissions from Indonesia, Africa and South America lead to the band of enhanced HCN in Fig. 4, extending from southern mid-latitudes to the northern subtropics in late 2006.

The year 2010 was characterised by very intensive biomass burning in South America, which in October caused a strong plume extending from Brazil to southern Africa with outflow towards Australia as well as to northern Africa (Fig. 6, bottom row). The HCN distribution of this month is in very good agreement with CO measured by MLS at the 147 hPa level (Liu et al., 2013, Fig. 8d). Referring to publications of Chen et al. (2011), Fernandes et al. (2011) and Lewis et al. (2011), these authors identify the severe drought in South America in 2010 as reason for the enhanced fire activity. According to these papers the drought resulted from a strong El Niño in 2009 and early 2010 and from a very warm tropical North Atlantic in 2010. In November the plume had somewhat diluted and spread out over the whole southern subtropical latitude band and to a lesser part over South Asia and the northern subtropics. In this year no significant biomass burning signatures from Indonesia were detected in the upper troposphere.

3.4.2 The Asian Monsoon Anticyclone

The AMA is a meteorological feature, which regularly occurs in the upper troposphere over southern Asia in June, July and August. It is a reservoir of air masses, in which pollutants from the northern subtropics are trapped and effectively transported high into the UTLS region (Randel et al., 2010). The HCN amounts measured by MIPAS inside the AMA also exhibited strong interannual variations. As illustration we show distributions at 16 km altitude of different years.

In July 2005 (Fig. 7, top left), HCN VMRs of up to 500 pptv were measured in the complete region covered by the anticyclone from the western Mediterranean to East Asia, while in July 2006 (top right) the HCN amounts in this area generally were 300–350 pptv only with a maximum slightly west of the center of the AMA. The area covered by enhanced HCN in July 2005 is in very good agreement with MLS observations of enhanced CO at 100 hPa ($\sim$ 16.5 km) (Liu et al., 2013, Fig. 5). In July 2007 and 2008 (middle row) the AMA contained nearly as high amounts of HCN as in 2005. A similar interannual variation of the HCN amounts inside the AMA was also observed by ACE-FTS (Randel et al., 2010, Fig. 3). As reason for the discrepancy between 2006 and the other years we assume release of different amounts of HCN into the northern subtropics during spring as source for subsequent upward transport inside the AMA. As illustration, HCN distributions at 12 km altitude from May 2005 and 2006 (botton row) show that in May 2005 the HCN amounts in the northern subtropical band were considerably higher than in May 2006. Substantial differences in the intensity of South and Southeast Asian biomass burning between the years 2005 and 2006 are consistent with HCN emission fluxes of the GFEDv2 biomass inventory, which in early 2005 were much higher than in early 2006 (Lupu et al., 2009, Fig. 1). At the western edge of the strongly polluted AMAs of 2005, 2007 and 2008 there is indication of southwestward transport of enhanced HCN towards the tropical Atlantic, which is a potential additional source of a tropical HCN tape recorder.

3.5 The tropical HCN tape recorder

As outlined in Sect. 1, a tropical tape recorder signal was found in MLS and ACE-FTS HCN data by Pumphrey et al. (2008). They detected a stratospheric cycle of 2 yr for the latitude band 15° S–15° N, but the time period investigated was rather short (mid-2004 to mid-2007). By analysis of ACE-FTS and MLS data and use of the GEOS-Chem model, Li et al. (2009) found a semi-annual and annual cycle in the upper troposphere and consecutive 2 year cycles in the lower stratosphere. The 2 year cycle for the time period investigated by Pumphrey et al. (2008) was also reproduced by model calculations of Pommrich et al. (2010), using Indonesian fires as lower boundary condition. However, since Indonesian biomass burning is strongly influenced by El Niño events, these authors assumed an irregular cycle for a longer time series. Thus the question of the, if any, dominant period in the HCN tape recorder signal is not yet fully answered and the long time series of MIPAS data can help to solve the problem.

First of all we checked if the signal derived by Pumphrey et al. (2008) can also be found in MIPAS data. The results of this test are presented in Fig. 8, which contains the MIPAS HCN "tape recorder signature" for the latitude band 15° S–15° N. In this presentation the mean values of the period are subtracted for each retrieval altitude. The presented time period is restricted to January 2005–June 2007, because there was an operational shutdown of MIPAS between April and December 2004. There is good agreement with the tape recorder signals derived from ACE-FTS and MLS HCN data (cf. Pumphrey et al., 2008, Fig. 1) in phase as well as in magnitude.

However, a re-inspection of Fig. 4 shows that the period investigated by these authors is not representative for the whole inner tropical HCN dataset of MIPAS, because it exhibits an extraordinarily strong upper tropospheric maximum at the end of 2006 caused by southern hemispheric and additional intensive biomass burning in Indonesia. On the other hand the northern tropical HCN maximum around May 2006 is nearly completely missing (there is only a weak maximum in the subtropics). The subse-

quent years 2007–2009 show a more regular pattern with alternating northern maxima around May and southern maxima around October–November.

For further illustration of the situation at tropical latitudes, Fig. 9 shows time series of monthly mean HCN at 14, 17, 20 and 23 km altitude, zonally-averaged over the latitude band 15° S–15° N. The most prominent signatures at 14 km are the strong maxima in November 2002, 2006 and 2010 (mind the data gap in 2004), caused by intensive biomass burning in the Southern Hemisphere and in Indonesia. Accordingly, the dominant period is an annual cycle with maxima in November. But there are also regular, generally weaker (due to the restriction to ±15°, cf. Fig. 4) maxima around April to May resulting from biomass burning in the Northern Hemisphere, which cause an overlapping semi-annual cycle. At 17 km altitude the November-maxima are considerably reduced. At 20 km there is an annual cycle with maxima in July and minima around February to April during the period 2007–2009. The amplitude of the cycle is much smaller than at lower altitudes (30 pptv at the most). Due to the reasons outlined above, there is no maximum in summer 2006 leading to a biennial cycle from mid-2005 to mid-2007. A similar, but not as distinctive biennial cycle is visible in the time period 2009–2011. As mentioned above, this temporal variation of HCN in the tropical lower stratosphere shows, that the period investigated by Pumphrey et al. (2008) is not representative for a longer time period. Obviously only the strongest maxima observed at 20 km altitude are transported to 23 km with a time shift of some months, while the weaker features are strongly damped.

Referring to Fig. 9, we also like to make a short note on MIPAS HCN at the tropical tropopause. The average HCN value at 17 km is 268 pptv, which seems to be sufficiently high to establish the stratospheric HCN amounts observed by MIPAS by tropical upwelling. For example, the mean value of the latitude band ±60° at 20 km altitude is 232 pptv. This result is different to the findings of Randel et al. (2010), who from analysis of ACE-FTS and MLS data conclude, that the HCN amounts at the tropical tropopause are too low for effective supply of stratospheric HCN and that stratospheric injection by the Asian monsoon anticyclone is essential.

To check for a tape recorder signal in the whole MIPAS HCN dataset, Fig. 10 (left) shows a time-height series of the inner tropics (15° S–15° N) from July 2002 to April 2012 after subtraction of the average value at each altitude. In addition, a three-month running mean has been applied to the time series. The upper tropospheric (10–17 km) HCN anomaly exhibits semi-annual to biennial cycles of considerably varying strength and a generally fast upward propagation. A stratospheric tape recorder signal becomes manifest in four bands of negative and positive anomalies, respectively. Vertical transport times in the lower stratosphere become considerably longer, e.g., about 9 months for the distance between 17 and 25 km altitude.

The first band of enhanced HCN entering the stratosphere covers the time period from end of 2002 to end of 2003 at the tropopause and arrives in the mid-stratosphere about half a year later (data gap). It is obviously initiated by southern hemispheric and Indonesian biomass burning and during 2003 enhanced by additional sources from central Africa and northern low latitudes. This band is followed by a negative anomaly extending from the end of 2003 to the end of 2004 at the tropopause and from mid 2004 to mid 2005 in the mid-stratosphere. The second positive anomaly extends from the uppermost troposphere in mid-2005 to the mid-stratosphere in mid-2006 and seems to be caused by the strong AMA of 2005. It is followed by a region with depleted HCN. The next band of enhanced stratospheric HCN is the strongest positive tape recorder signal observed in MIPAS HCN, extending from autumn 2006 to the end of 2007 at 17 km and from mid-2007 to the end of 2008 at 25 km altitude. This anomaly is caused by accumulation of HCN released by biomass burning during the whole period autumn 2006 to May 2008, namely strong pollution from the southern hemispheric plume and Indonesia at the end of 2006, from central Africa in spring 2007 and a strong AMA with effusion into the tropical latitude band and southern hemispheric biomass burning in summer 2007. Thereupon follows a period with depleted HCN from the end of 2008 until autumn 2010 at 17 km, caused by upper tropospheric HCN deficits in early 2008, 2009 and most of 2010. This signal re-appears at 25 km altitude from spring 2009 until autumn 2011. The positive anomaly of autumn 2009 could not propagate into the

stratosphere. The next period of enhanced stratospheric HCN lasts from autumn 2010 to the end of 2011 at 17 km and from autumn 2011 to the end of the observation period at 25 km altitude. This anomaly is created by combination of sources from the unusually strong biomass burning at the end of 2010 in South America, from the Asian monsoon in 2011 and from southern hemispheric biomass burning at the end of 2011.

The development of the strong tape recorder signal of 2007 is illustrated in Fig. 11 by HCN distributions at 20 km altitude. In October 2006 (top left) fresh pollution has not yet reached this high altitude and the HCN VMRs in the whole tropical latitude band amount to about 240 pptv. In January (top right) large tropical areas contain enhanced (up to 280 pptv) amounts of HCN, which were released by southern hemispheric and Indonesian biomass burning. Refreshed by biomass burning in central Africa, enhanced HCN covers the whole tropical latitude band in May 2007 (bottom left). The distribution of July 2007 (bottom right) shows the additional contribution of the Asian monsoon.

In summary, the HCN anomaly exhibits semi-annual to annual cycles in the troposphere, which in the stratosphere are replaced by two consecutive biennial cycles with maxima in the lowermost stratosphere in mid-2003, mid-2005 and mid-2007. However, as outlined above, we think the apparent biennial cycle is caused by interannual variations in biomass burning and does not have a direct meteorological reason beyond the effect of meteorology on the biomass burning itself. These maxima propagate upward to 25 km within about 9 months. This feature is in good agreement with tropical HCN anomalies of the GEOS-Chem model presented by Li et al. (2009, Fig. 6). After 2007 this regular pattern is disrupted. At 19 km there are two weak maxima in 2008 and 2009. The first of these maxima apparently merges with the preceding maximum of 2007 in the middle stratosphere, and the second is too weak to propagate further upward. In mid-2011 the biennial cycle obviously is resumed again with a positive anomaly propagating upward into the stratosphere. Effective upward propagation of positive HCN anomalies into the stratosphere obviously occurs during periods of extensive southern hemispheric and Indonesian biomass burning followed by a strong AMA containing

large amounts of HCN, because a certain portion of this high HCN is released into the tropical belt at its western edge.

For comparison with another tropospheric tracer, Fig. 10 (right) shows the water vapour tape recorder signal derived from MIPAS measurements. Due to a dominant seasonal cycle and lower interannual variations of the water vapour anomaly at the tropopause, the H_2O tape recorder exhibits a rather regular annual cycle. Apart from the different tape recorder periods, the vertical stratospheric transport velocity visible in the temporal shift of the H_2O anomalies with increasing altitude obviously agrees quite well with the stratospheric vertical speed observed in HCN.

A more quantitative estimation of vertical transport times can be performed by means of Fig. 9. The time lag between the maxima at 14 and 17 km in the troposphere is generally 0–1 months only. The time shift for upward transport of the strongest stratospheric maxima at 20 km in 2003, 2005 and 2007 to the altitude of 23 km is 5–6 months, which is considerably longer. For comparison, the time lags between MLS CO maxima at 147 and 68 hPa (about 14.3 and 19 km altitude) published by Liu et al. (2013) are 0–2 months for northern hemispheric and 3–4 months for southern hemispheric fires.

4   Conclusions

We have presented a climatology of MIPAS HCN data, covering the period June 2002 to April 2012, as well as interannual variations with the focus on the tropical and subtropical upper troposphere and lower stratosphere. HCN is a nearly unique tracer of biomass burning with a tropospheric lifetime of 5–6 months, which is short enough to observe seasonal and annual differences in fire activity and long enough to study long-range and vertical transport. The highest low-latitude upper tropospheric HCN amounts were generally detected during October and November in the southern tropics and subtropics, caused by biomass burning in South America, southern Africa and, in the years 2002 and 2006 with a high ENSO-index, by strong burning activity in Indonesia and northern Australia. The highest low-latitude northern HCN amounts were

measured from June to August inside the Asian monsoon anticyclone. During boreal summer high HCN amounts were also observed at northern mid- and high latitudes. Possibly due to ocean uptake (Li et al., 2000, 2003; Singh et al., 2003) the upper tropospheric background amounts exhibit a minimum above the tropical and subtropical

5   oceans, which is most pronounced during boreal winter and spring. The HCN climatology obtained from ACE-FTS data exhibits a similar seasonal variation, but the HCN amounts derived from MIPAS data are generally higher by about 50 pptv.

Time series of upper tropospheric HCN data show a regular annual period with maxima in October/November in the southern tropics and subtropics. However, the maxi-

10 mum volume mixing ratios exhibit distinct interannual variations between 300 and more than 500 pptv (monthly means), reflecting varying burning activities in South America, southern Africa and Indonesia/northern Australia. The fundamental period at northern low- to mid-latitudes is also an annual cycle, which in the tropics peaks in April/May during the North African and South Asian biomass burning season and in the subtropics

15 around July due to trapping of pollutants in the Asian monsoon anticyclone. In several years this cycle is considerably disturbed, either by additional maxima in autumn 2002, 2006 and 2010 resulting from biomass burning in Indonesia and in northern Africa or by nearly complete absence of the springtime maximum like in 2006. The HCN amounts measured in the upper troposphere exhibit negative trends, e.g. at 10 km altitude −1.3

20 to −2.1 % yr^{-1} in the northern and and −0.1 to −0.7 % yr^{-1} in the Southern Hemisphere. The significance of these trends will be investigated in more detail in future analysis. Enhanced HCN released by tropical and subtropical biomass burning is subsequently transported to high latitudes. The average transport time in the Southern Hemisphere is about 1.6 months. Due to overlapping signatures from the northern and Southern

25 Hemisphere the equatorial upper troposphere generally exhibits a semi-annual cycle. This feature is replaced by an annual or, caused by the disturbances mentioned above, even biennial cycle peaking around July in the tropical lower stratosphere. There is a time shift of some months between the upper tropospheric and lower stratospheric maxima. MIPAS HCN data do not show such a strong predominance of the Asian mon-

soon anticyclone as source of stratospheric HCN as found by Randel et al. (2010) from analysis of ACE-FTS and MLS data.

The apparently biennial HCN tape recorder signal in the tropical stratosphere derived by Pumphrey et al. (2008) from MLS and ACE-FTS data of the time period mid-2004 to mid-2007 agrees well with that derived from MIPAS data of this period. While annual or semi-annual cycles prevail in the upper troposphere, lower stratospheric variations in the whole MIPAS dataset exhibit lower frequencies, including periodicities of 2 and 4 yr. These periodicities, however, do not have a direct meteorological reason, but are rather introduced by source strength variations. Strong positive anomalies transported upward into the stratosphere are a combination of enhanced HCN from southern hemispheric and Indonesian biomass burning at the end of the year and from the Asian monsoon during the subsequent summer. Vertical transport of the anomalies is rather fast in the upper troposphere but considerably slower in the stratosphere, e.g. 0–1 months from 14 to 17 km and about 9 months from 17 to 25 km altitude.

References

Andrews, A. E., Boering, K. A., Daube, B. C., Wofsy, S. C., Hintsa, E. J., Weinstock, E. M., and Bui, T. P.: Empirical age spectra for the lower tropical stratosphere from in situ observations of CO_2: implications for stratospheric transport, J. Geophys. Res., 104, 26581–26595, 1999.
Chen, Y., Randerson, J. T., Morton, D. C., DeFries, R. S., Collatz, G. J., Kasibhatla, P. S., Giglio, L., Jin, Y. F., and Marlier, M. E.: Forecasting fire season sever-

ity in South America using sea surface temperature anomalies, Science, 334, 787–791, doi:10.1126/science.1209472, 2011.

Cicerone, R. J. and Zellner, R.: The atmospheric chemistry of hydrogen cyanide (HCN), J. Geophys. Res., 88, 10689–10696, 1983.

5 Coffey, M. T., Mankin, W. G., and Cicerone, R. J.: Spectroscopic detection of stratospheric hydrogen cyanide, Science, 214, 333–335, 1981.

European Space Agency: Envisat, MIPAS An instrument for atmospheric chemistry and climate research, ESA Publications Division, ESTEC, P.O. Box 299, 2200 AG Noordwijk, The Netherlands, SP-1229, 2000.

10 Fernandes, K., Baethgen, W., Bernardes, S., DeFries, R., DeWitt, D. G., Goddard, L., Lavado, W., Lee, D. E., Padoch, C., Pinedo-Vasquez, M., and Uriarte, M.: North Tropical Atlantic influence on western Amazon fire season variability, Geophys. Res. Lett., 38, L12701, doi:10.1029/2011gl047392, 2011.

Fischer, H., Birk, M., Blom, C., Carli, B., Carlotti, M., von Clarmann, T., Delbouille, L., Dud-

15 hia, A., Ehhalt, D., Endemann, M., Flaud, J. M., Gessner, R., Kleinert, A., Koopman, R., Langen, J., López-Puertas, M., Mosner, P., Nett, H., Oelhaf, H., Perron, G., Remedios, J., Ridolfi, M., Stiller, G., and Zander, R.: MIPAS: an instrument for atmospheric and climate research, Atmos. Chem. Phys., 8, 2151–2188, doi:10.5194/acp-8-2151-2008, 2008.

Glatthor, N., von Clarmann, T., Stiller, G. P., Funke, B., Koukouli, M. E., Fischer, H.,

20 Grabowski, U., Höpfner, M., Kellmann, S., and Linden, A.: Large-scale upper tropospheric pollution observed by MIPAS HCN and C_2H_6 global distributions, Atmos. Chem. Phys., 9, 9619–9634, doi:10.5194/acp-9-9619-2009, 2009.

Höpfner, M., von Clarmann, T., Fischer, H., Glatthor, N., Grabowski, U., Kellmann, S., Kiefer, M., Linden, A., Mengistu Tsidu, G., Milz, M., Steck, T., Stiller, G. P., Wang, D.-Y., and Funke, B.:

25 First spaceborne observations of Antarctic stratospheric $ClONO_2$ recovery: austral spring 2002, J. Geophys. Res., 109, D11308, doi:10.1029/2004JD004609, 2004.

Holton, J. R., Haynes, P. H., McIntyre, M. E., Douglass, A. R., Rood, R. B., and Pfister, L.: Stratosphere–troposphere exchange, Rev. Geophys., 33, 403–439, 1995.

Lewis, S. L., Brando, P. M., Phillips, O. L., van der Heijden, G. M. F., and Nepstad, D.: The 2010

30 Amazon drought, Science, 331, 554–554, doi:10.1126/science.1200807, 2011.

Li, Q., Jacob, D. J., Bey, I., Yantosca, R. M., Zhao, Y., Kondo, Y., and Notholt, J.: Atmospheric hydrogen cyanide (HCN): biomass burning source, ocean sink?, Geophys. Res. Lett., 27, 357–360, 2000.

Li, Q., Jacob, D. J., Yantosca, R. M., Heald, C. L., Singh, H. B., Koike, M., Zhao. Y., Sachse, G. W., and Streets, D. G.: A global three-dimensional model analysis of the atmospheric budgets of HCN and CH_3CN: constraints from aircraft and ground measurements, J. Geophys. Res., 108, 8827, doi:10.1029/2002JD003075, 2003.

5 Li, Q., Palmer, P. I., Pumphrey, H. C., Bernath, P., and Mahieu, E.: What drives the observed variability of HCN in the troposphere and lower stratosphere?, Atmos. Chem. Phys., 9, 8531–8543, doi:10.5194/acp-9-8531-2009, 2009.

Liu, J., Logan, J. A., Murray, L. T., Pumphrey, H. C., Schwartz, M. J., and Megretskaia, I. A.: Transport analysis and source attribution of seasonal and interannual variability of CO in
10 the tropical upper troposphere and lower stratosphere, Atmos. Chem. Phys., 13, 129–146, doi:10.5194/acp-13-129-2013, 2013.

Lupu, A., Kaminski, J. W., Neary, L., McConnell, J. C., Toyota, K., Rinsland, C. P., Bernath, P. F., Walker, K. A., Boone, C. D., Nagahama, Y., and Suzuki, K.: Hydrogen cyanide in the upper troposphere: GEM-AQ simulation and comparison with ACE-FTS observations, Atmos.
15 Chem. Phys., 9, 4301–4313, doi:10.5194/acp-9-4301-2009, 2009.

Mahieu, E., Rinsland, C. P., Zander, R., Demoulin, P., Delbouille, L., and Roland, G.: Vertical column abundances of HCN deduced from ground-based infrared solar spectra: long-term trend and variability, J. Atmos. Chem., 20, 299–310, 1995.

Mahieu, E., Zander, R., Delbouille, L., Demoulin, P., Roland, G., and Servais, C.: Observed
20 trends in total vertical column abundances of atmospheric gases from IR solar spectra recorded at the Jungfraujoch, J. Atmos. Chem., 28, 227–243, 1997.

Morgenstern, O., Zeng, G., Wood, S. W., Robinson, J., Smale, D., Paton-Walsh, C., Jones, N. B., and Griffith, D. W. T.: Long-range correlations in Fourier transform infrared, satellite, and modeled CO in the Southern Hemisphere, J. Geophys. Res., 117, D11301,
25 doi:10.1029/2012JD017639, 2012.

Mote, P. W., Rosenlof, K. H., McIntyre, M. E., Carr, E. S., Gille, J. C., Holton, J. R., Kinnersley, J. S., Pumphrey, H. C., Russell, J. M., and Waters, J. W.: An atmospheric tape recorder: the imprint of tropical tropopause temperatures on stratospheric water vapor, J. Geophys. Res., 101, 3989–4006, 1996.

30 Nett, H., Perron, G., Sanchez, M., Burgess, A., and Mossner, P.: MIPAS inflight calibration and processor validation, in ENVISAT Calibration Review – Proc. of the European Workshop, 9–13 September 2002, ESTEC, Noordwijk, the Netherlands, CD-ROM, vol. SP-520, edited by: Sawaya-Lacoste, H., ESA Publications Division, ESTEC, Noordwijk, the Netherlands, 2002.

Title Page

Abstract | Introduction

Conclusions | References

Tables | Figures

|◄ | ►|

◄ | ►

Back | Close

Full Screen / Esc

Printer-friendly Version

Interactive Discussion

Park, M., Randel, W. J., Emmons, L. K., Bernath, P. F., Walker, K. A., and Boone, C. D.: Chemical isolation in the Asian monsoon anticyclone observed in Atmospheric Chemistry Experiment (ACE-FTS) data, Atmos. Chem. Phys., 8, 757–764, doi:10.5194/acp-8-757-2008, 2008.

Pommrich, R., Müller, R., Grooß, J. U., Günther, G., Konopka, P., Riese, M., Heil, A., Schultz, M., Pumphrey, H. C., and Walker, K. A.: What causes the irregular cycle of the atmospheric tape recorder signal in HCN?, Geophys. Res. Lett, 37, L16805, doi:10.1029/2010GL044056, 2010.

Pumphrey, H. C., Jimenez, C. J., and Waters, J. W.: Measurement of HCN in the middle atmosphere by EOS MLS, Geophys. Res. Lett., 33, L08804, doi:10.1029/2005GL025656, 2006.

Pumphrey, H. C., Boone, C., Walker, K. A., Bernath, P., and Livesey, N. J.: Tropical tape recorder observed in HCN, Geophys. Res. Lett, 35, L05801, doi:10.1029/2007GL032137, 2008.

Randel, W. J., Park, M., Emmons, L., Kinnison, D., Bernath, P., Walker, K. A., Boone, C., and Pumphrey, H.: Asian Monsoon transport of pollution to the stratosphere, Science, 328, 611, doi:10.1126/science.1182274, 2010.

Remedios, J. J., Leigh, R. J., Waterfall, A. M., Moore, D. P., Sembhi, H., Parkes, I., Greenhough, J., Chipperfield, M.P., and Hauglustaine, D.: MIPAS reference atmospheres and comparisons to V4.61/V4.62 MIPAS level 2 geophysical data sets, Atmos. Chem. Phys. Discuss., 7, 9973–10017, doi:10.5194/acpd-7-9973-2007, 2007.

Rinsland, C. P., Smith, M. A. H., Rinsland, P. L., Goldman, A., Brault, J. W., and Stokes, G. M.: Ground-based spectroscopic measurements of atmospheric hydrogen cyanide, J. Geophys. Res., 87, 11119–11125, 1982.

Rinsland, C. P., Gunson, M. R., Wang, P.-H., Arduini, R. F., Baum, B. A., Minnis, P., Goldman, A., Abrams, M. C., Zander, R., Mahieu, E., Salawitch, R. J., Michelsen, H. A., Irion, F. W., and Newchurch, M. J.: ATMOS/ATLAS 3 infrared measurements of trace gases in the November 1994 tropical and subtropical upper troposphere, J. Quant. Spectrosc. Ra., 60, 891–901, 1998.

Rinsland, C. P., Goldman, A., Murcray, F. J., Stephen, T. M., Pougatchev, N. S., Fishman, J., David S. J., Blatherwick, R. D., Novelli, P. C., Jones, N. B., and Connor, B. J.: Infrared solar spectroscopic measurements of free tropospheric CO, C_2H_6, and HCN above Mauna Loa, Hawaii: seasonal variations and evidence for enhanced emissions from the southeast Asian tropical fires of 1997–1998, J. Geophys. Res., 104, 18667–18680, 1999.

Rinsland, C. P., Mahieu, E., Zander, R., Demoulin, P., Forrer, J., and Buchmann, B.: Free tropospheric CO, C_2H_6, and HCN above central Europe: recent measurements from the Jungfraujoch station including the detection of elevated columns during 1998, J. Geophys. Res., 105, 24235–24249, 2000.

5 Rinsland, C. P., Goldman, A., Zander, R., and Mahieu, E.: Enhanced tropospheric HCN columns above Kitt Peak during the 1982–1983 and 1997–1998 El Niño warm phases, J. Quant. Spectrosc. Ra., 69, 3–8, 2001a.

Rinsland, C. P., Meier, A., Griffith, D. W. T., and Chiou, L. S.: Ground-based measurements of tropospheric CO, C_2H_6, and HCN from Australia at 34° S latitude during 1997–1998, J.

10 Geophys. Res., 106, 20913–20924, 2001b.

Rinsland, C. P., Jones, N. B., Connor, B. J., Wood, S. W., Goldman, A., Stephen, T. M., Murcray, F. J., Chiou, L. S., Zander, R., and Mahieu, E.: Multiyear infrared solar spectroscopic measurements of HCN, CO, C_2H_6, and C_2H_2 tropospheric columns above Lauder, New Zealand (45° S latitude), J. Geophys. Res., 107, 4185, doi:10.1029/2001JD001150, 2002.

15 Rinsland, C. P., Dufour, G., Boone, C. D., and Bernath, P. F.: Atmospheric Chemistry Experiment (ACE) measurements of elevated Southern Hemisphere upper tropospheric CO, C_2H_6, HCN, and C_2H_2 mixing ratios from biomass burning emissions and long range transport, Geophys. Res. Lett., 32, L20803, doi:10.1029/2005GL024214, 2005.

Schoeberl, M. R., Duncan, B. N., Douglass, A. R., Waters, J., Livesey, N., Read, W.,

20 and Filipiak, M.: The carbon monoxide tape recorder, Geophys. Res. Lett., 33, L12811, doi:10.1029/2006GL026178, 2006.

Singh, H. B., Herlth, D., Kolyer, R., Chatfield, R., Viezee, W., Salas, L. J., Chen, Y., Bradshaw, J. D., Sandholm, S. T., Talbot, R., Gregory, G. L., Anderson, B., Sachse, G. W., Browell, E., Bachmeier, A. S., Blake, D. R., Heikes, B., Jacob, D., and H. E. Fuelberg: Impact of

25 biomass burning emissions on the composition of the South Atlantic troposphere: reactive nitrogen and ozone, J. Geophys. Res., 101, 24203–24219, 1996.

Singh, H. B., Viezee, W., Chen, Y., Bradshaw, J., Sandholm, S., Blake, D., Blake, N., Heikes, B., Snow, J., Talbot, R., Browell, E., Gregory, G., Sachse, G., and Vay, S.: Biomass burning influences on the composition of the remote South Pacific troposphere: analysis based on

30 observations from PEM-Tropics-A, Atmos. Environ., 34, 635–644, 2000.

Singh, H. B., Salas, L., Herlth, D., Kolyer, R., Czech, E., Viezee, W., Li, Q., Jacob, D. J., Blake, D., Sachse, G., Harward, C. N., Fuelberg, H., Kiley, C. M., Zhao, Y., and Kondo, Y.: In situ

Variations of MIPAS HCN amounts

N. Glatthor et al.

Title Page

Abstract | Introduction

Conclusions | References

Tables | Figures

|◀ | ▶|

◀ | ▶

Back | Close

Full Screen / Esc

Printer-friendly Version

Interactive Discussion

measurements of HCN and CH$_3$CN over the Pacific Ocean: sources, sinks and budgets, J. Geophys. Res., 108, 8795, doi:10.1029/2002JD003006, 2003.

Steck, T.: Methods for determining regularization for atmospheric retrieval problems, Appl. Optics, 41, 1788–1797, 2002.

Stiller, G. P. (Ed.): The Karlsruhe Optimized and Precise Radiative transfer Algorithm (KOPRA), Wissenschaftliche Berichte, vol. FZKA 6487, Forschungszentrum Karlsruhe GmbH, 2000.

von Clarmann, T., Fischer, H., Funke, B., Glatthor, N., Grabowski, U., Höpfner, M., Kellmann, S., Kiefer, M., Linden, A., Mengistu Tsidu, G., Milz, M., Steck, T., Stiller, G. P., Wang, D.-Y., Gil-López, S., and López-Puertas, M.: Retrieval of temperature and tangent altitude pointing from limb emission spectra recorded from space by the Michelson Interferometer for Passive Atmospheric Sounding (MIPAS), J. Geophys. Res., 108, doi:10.1029/2003JD003602, 2003.

von Clarmann, T., Glatthor, N., Koukouli, M. E., Stiller, G. P., Funke, B., Grabowski, U., Höpfner, M., Kellmann, S., Linden, A., Milz, M., Steck, T., and Fischer, H.: MIPAS measurements of upper tropospheric C$_2$H$_6$ and O$_3$ during the southern hemispheric biomass burning season in 2003, Atmos. Chem. Phys., 7, 5861–5872, doi:10.5194/acp-7-5861-2007, 2007.

von Clarmann, T., Höpfner, M., Kellmann, S., Linden, A., Chauhan, S., Funke, B., Grabowski, U., Glatthor, N., Kiefer, M., Schieferdecker, T., Stiller, G. P., and Versick, S.: Retrieval of temperature, H$_2$O, O$_3$, HNO$_3$, CH$_4$, N$_2$O, ClONO$_2$ and ClO from MIPAS reduced resolution nominal mode limb emission measurements, Atmos. Meas. Tech., 2, 159–175, doi:10.5194/amt-2-159-2009, 2009.

van der Werf, G. R., Randerson, J. T., Giglio, L., Collatz, G. J., Kasibhatla, P. S., and Arellano Jr., A. F.: Interannual variability in global biomass burning emissions from 1997 to 2004, Atmos. Chem. Phys., 6, 3423–3441, doi:10.5194/acp-6-3423-2006, 2006.

van der Werf, G. R., Randerson, J. T., Giglio, L., Collatz, G. J., Mu, M., Kasibhatla, P. S., Morton, D. C., DeFries, R. S., Jin, Y., and van Leeuwen, T. T.: Global fire emissions and the contribution of deforestation, savanna, forest, agricultural, and peat fires (1997–2009), Atmos. Chem. Phys., 10, 11707–11735, doi:10.5194/acp-10-11707-2010, 2010.

Wiegele, A., Glatthor, N., Höpfner, M., Grabowski, U., Kellmann, S., Linden, A., Stiller, G., and von Clarmann, T.: Global distributions of C$_2$H$_6$, C$_2$H$_2$, HCN, and PAN retrieved from MIPAS reduced spectral resolution measurements, Atmos. Meas. Tech., 5, 723–734, doi:10.5194/amt-5-723-2012, 2012.

Worden, H. M., Deeter, M. N., Frankenberg, C., George, M., Nichitiu, F., Worden, J., Aben, I., Bowman, K. W., Clerbaux, C., Coheur, P. F., de Laat, A. T. J., Detweiler, R., Drummond, J. R.,

Title Page

Abstract | Introduction

Conclusions | References

Tables | Figures

|◄ | ►|

◄ | ►

Back | Close

Full Screen / Esc

Printer-friendly Version

Interactive Discussion

Edwards, D. P., Gille, J. C., Hurtmans, D., Luo, M., Martínez-Alonso, S., Massie, S., Pfister, G., and Warner, J. X.: Decadal record of satellite carbon monoxide observations, Atmos. Chem. Phys., 13, 837–850, doi:10.5194/acp-13-837-2013, 2013.

Yokelson, R. J., Urbanski, S. P., Atlas, E. L., Toohey, D. W., Alvarado, E. C., Crounse, J. D., Wennberg, P. O., Fisher, M. E., Wold, C. E., Campos, T. L., Adachi, K., Buseck, P. R., and Hao, W. M.: Emissions from forest fires near Mexico City, Atmos. Chem. Phys., 7, 5569–5584, doi:10.5194/acp-7-5569-2007, 2007.

Zeng, G., Wood, S. W., Morgenstern, O., Jones, N. B., Robinson, J., and Smale, D.: Trends and variations in CO, C_2H_6, and HCN in the Southern Hemisphere point to the declining anthropogenic emissions of CO and C_2H_6, Atmos. Chem. Phys., 12, 7543–7555, doi:10.5194/acp-12-7543-2012, 2012.

Title Page

Abstract | Introduction

Conclusions | References

Tables | Figures

|◄ | ►|

◄ | ►

Back | Close

Full Screen / Esc

Printer-friendly Version

Interactive Discussion

Table 1. Time shift in months between the HCN maxima observed at 10 km altitude in the southern hemispheric latitude bands 0–30° S and 60–90° S for the different years of the operational period of MIPAS. Due to data gaps, time shifts could not be derived for the years 2004 and 2005.

Year	Time shift [months]
2002	3
2003	0–3
2004	–
2005	–
2006	3
2007	1
2008	0
2009	2
2010	1
2011	1
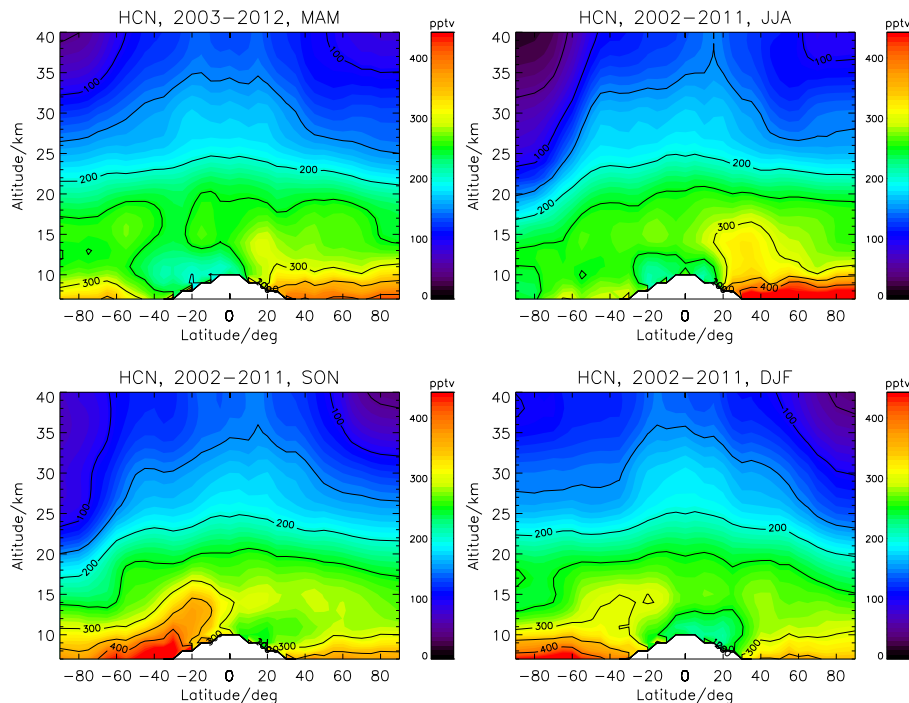
Fig. 1. Climatological latitude-height cross sections of HCN volume mixing ratios measured by MIPAS during March to May (top left), June to August (top right), September to November (bottom left) and December to February (bottom right). The distributions are averaged over the time period 2002 to 2012.

Title Page

Abstract | Introduction

Conclusions | References

Tables | Figures

|◄ | ►|

◄ | ►

Back | Close

Full Screen / Esc

Printer-friendly Version

Interactive Discussion
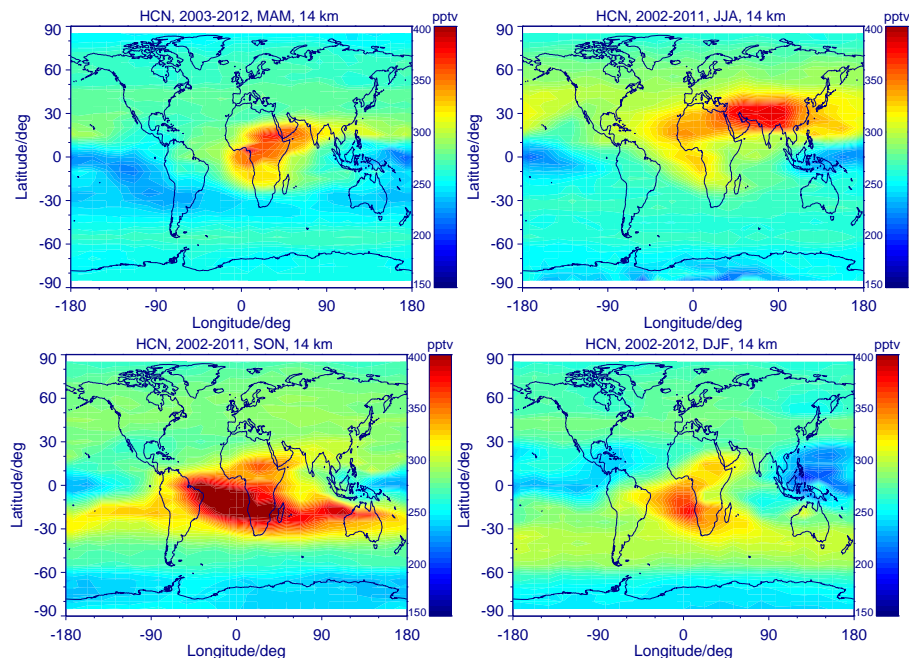
Fig. 2. Climatological global HCN distributions measured by MIPAS during March to May (top left), June to August (top right), September to November (bottom left) and December to February (bottom right) at 14 km altitude. The distributions are averaged over the time period 2002 to 2012. Here and in subsequent contour plots values exceeding the displayed VMR-range are also displayed in dark red.
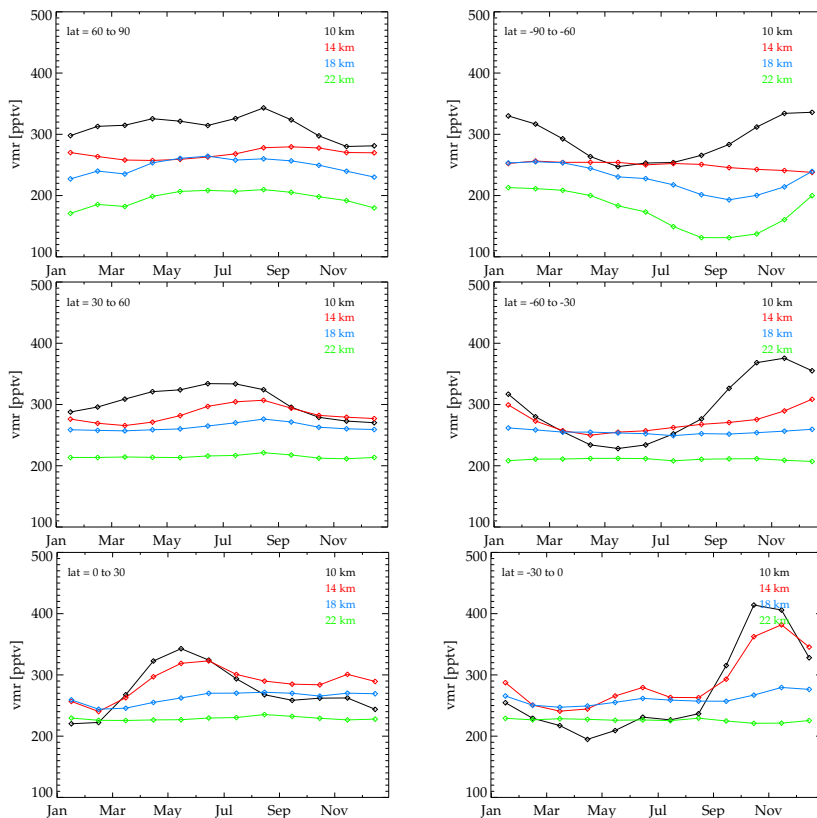
Fig. 3. Climatological monthly mean HCN volume mixing ratios measured by MIPAS at the altitudes of 10 (black), 14 (red), 18 (blue) and 22 km (green) in the latitude bands 60–90° (top row), 30–60° (middle row) and 0–30° (bottom row) for the Northern (left column) and Southern Hemisphere (right column). The monthly means are averaged over the time period 2002 to 2012.

Title Page

Abstract | Introduction

Conclusions | References

Tables | Figures

◀ | ▶|

◀ | ▶

Back | Close

Full Screen / Esc

Printer-friendly Version

Interactive Discussion
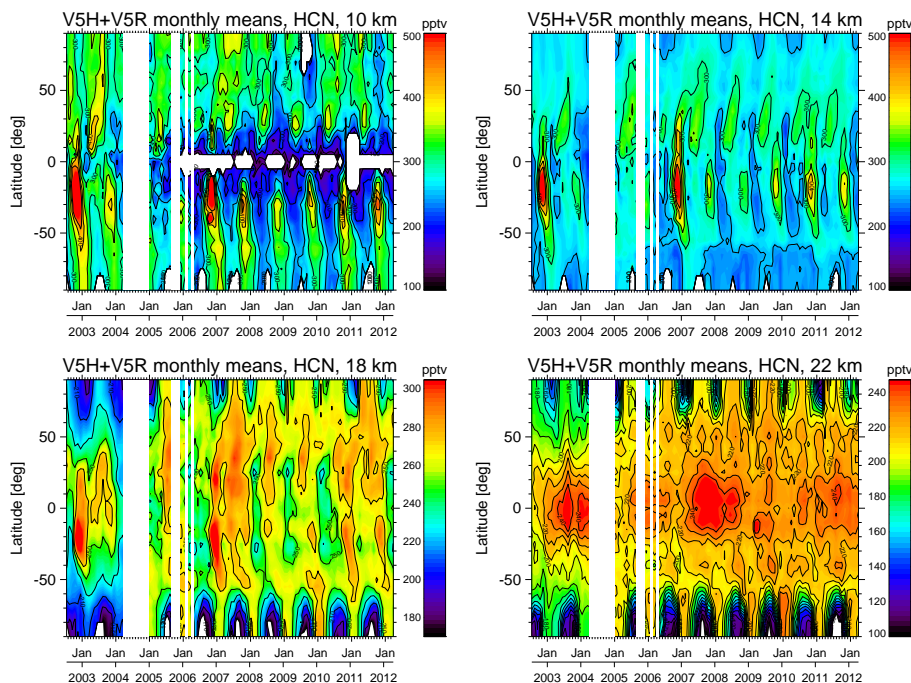
Fig. 4. Time series of monthly and zonally averaged HCN measured by MIPAS at 10 km (top left), 14 km (top right), 18 km (bottom left) and 22 km altitude (bottom right). White areas extending over the whole latitude range are data gaps due to operational shutdown of MIPAS, white areas after mid-2005 at 10 km in the equatorial region are caused by upward shift of the RR mode limb-scans towards low latitudes. Note the changed VMR-scales in the bottom row.
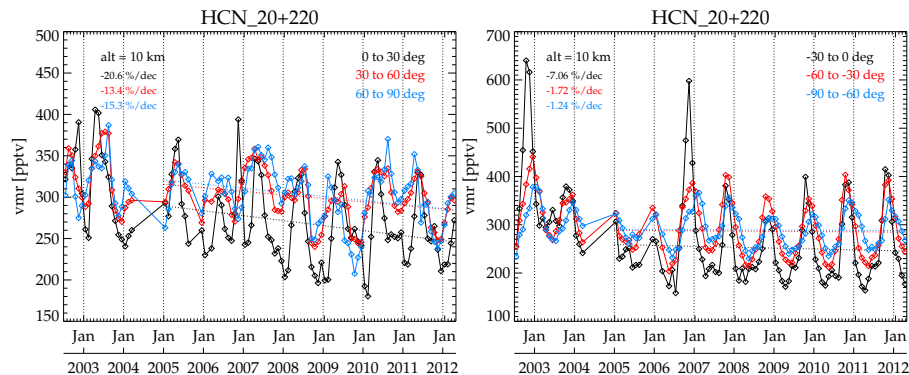
Fig. 5. Left: time series of monthly mean HCN measured by MIPAS at 10 km altitude in the latitude bands 0–30° N (black), 30–60° N (red) and 60–90° N (blue). Right: same as left, but for the latitude bands 0–30° S (black), 30–60° S (red) and 60–90° S (blue). Dashed lines are linear trends fitted to the data in the different latitude bands.
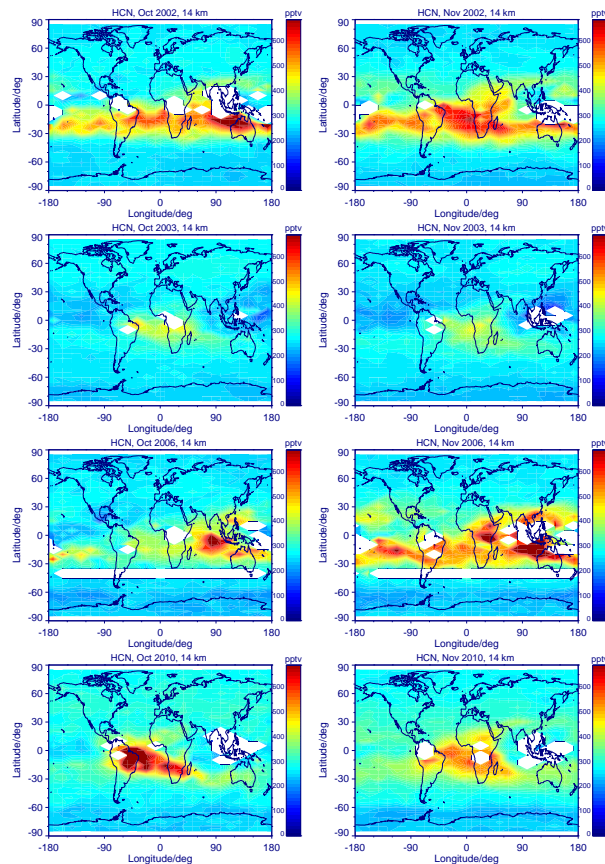
Fig. 6. Left column: global distribution of HCN measured by MIPAS at 14 km altitude in October 2002 (top), October 2003 (second row), October 2006 (third row) and October 2010 (bottom). Right column: same as left, but for November 2002, 2003, 2006 and 2010. White ares contain no measurements due to cloud contamination or discontinuities in the scan pattern (horizontal stripe).

Title Page

Abstract | Introduction

Conclusions | References

Tables | Figures

Back | Close

Full Screen / Esc

Printer-friendly Version

Interactive Discussion
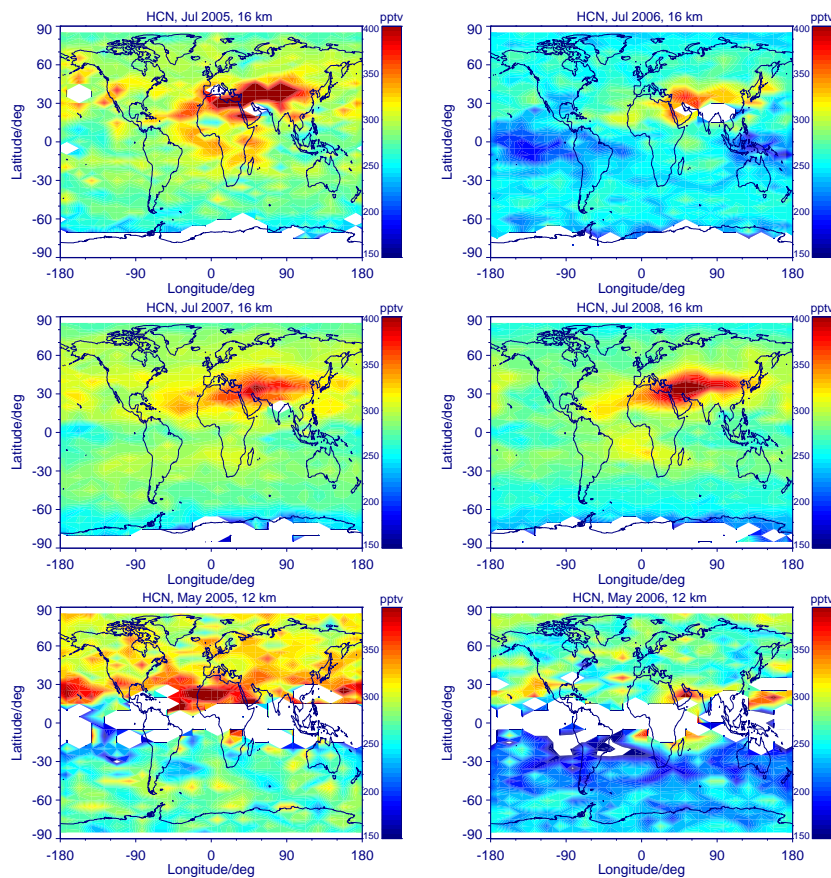
Fig. 7. Global HCN distributions measured by MIPAS at 16 km altitude during the peak of the Asian Monsoon Anticyclone in July 2005 and 2006 (top row) and July 2007 and 2008 (middle row) and measured at 12 km in May 2005 and 2006 (bottom row).

Title Page

Abstract | Introduction

Conclusions | References

Tables | Figures

◄ | ►

◄ | ►

Back | Close

Full Screen / Esc

Printer-friendly Version

Interactive Discussion

HCN anomaly, 15S-15N
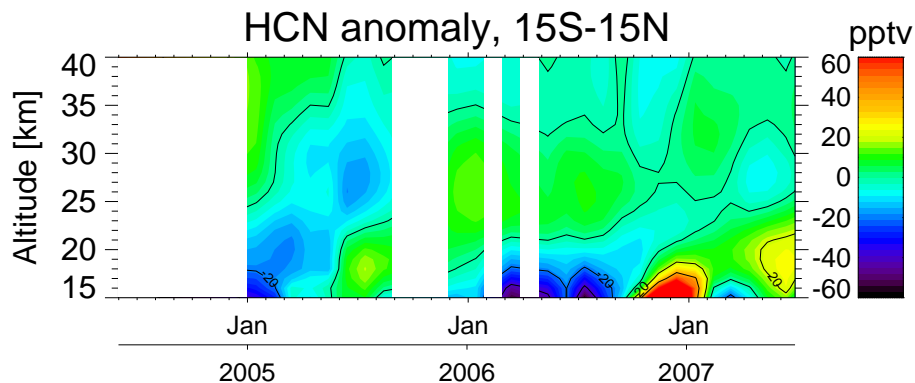
Fig. 8. Time series of monthly averaged HCN measured by MIPAS in the latitude band 15° S–15° N from January 2005 to June 2007. The average HCN VMR of each altitude has been subtracted. White areas are data gaps.
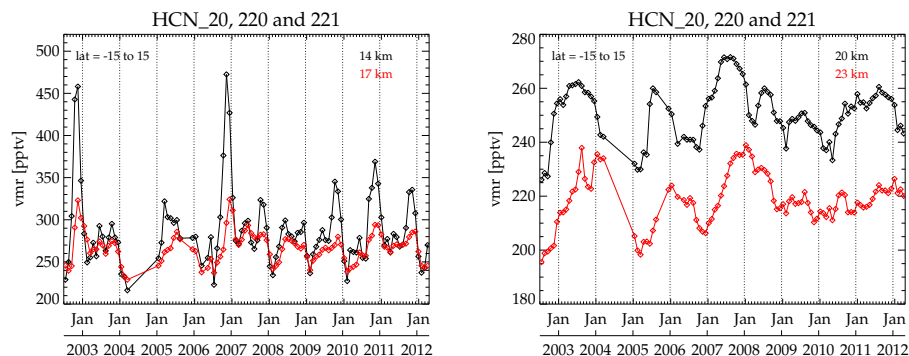
Fig. 9. Time series of monthly mean HCN measured by MIPAS at 14 and 17 km (left) and at 20 and 23 km altitude (right), zonally-averaged over the latitude band 15° S–15° N.
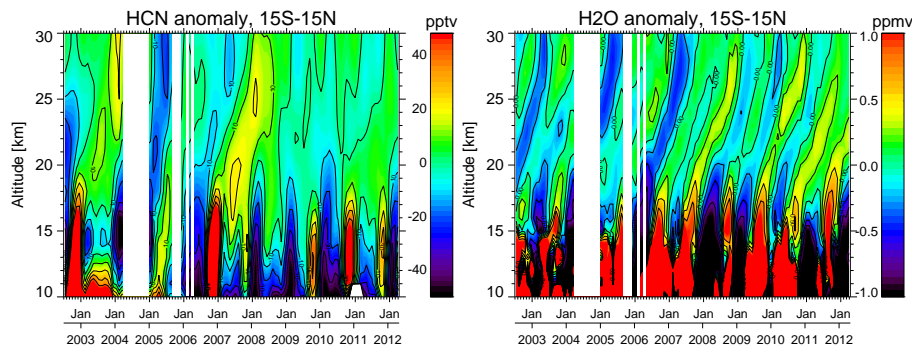
Fig. 10. Left: time series of monthly averaged HCN measured by MIPAS in the latitude band 15° S–15° N from July 2002 to April 2012. The average HCN VMR of each altitude has been subtracted. White areas are data gaps. Right: same as left, but for MIPAS H$_2$O.

Title Page

Abstract | Introduction

Conclusions | References

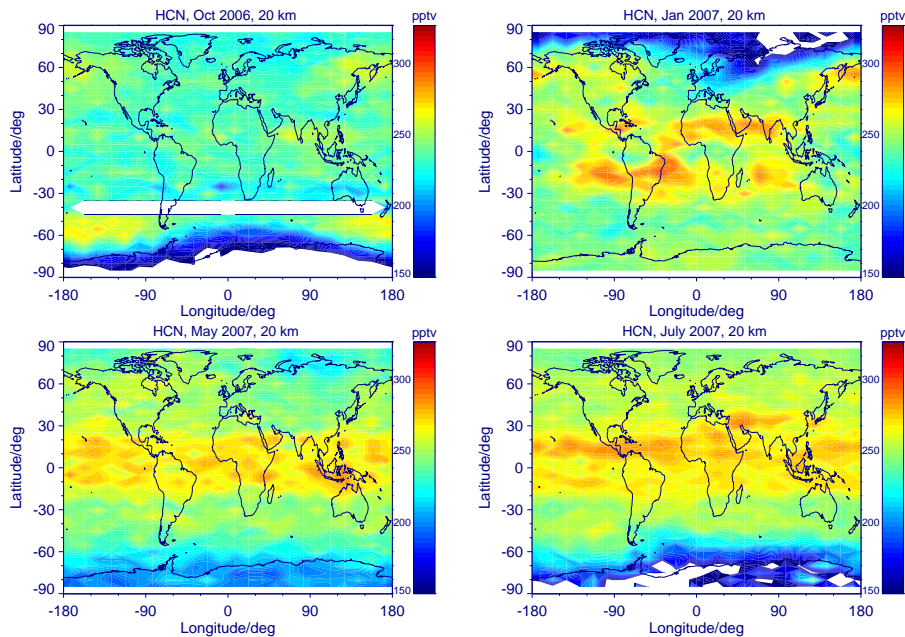Tables | Figures

|◄ | ►|

◄ | ►

Back | Close

Full Screen / Esc

Printer-friendly Version

Interactive Discussion

Fig. 11. Global HCN distributions measured by MIPAS at 20 km altitude during October 2006 (top left), January 2007 (top right), May 2007 (bottom left) and July 2007 (bottom right).